ISSN: 2688-8645

The Design and Analysis of the Fully Smooth Rotor Profile of Twin-Screw Vacuum Pump

Yongqi Li, Wang Xu, Yichao Sun, Yuefei Zheng

School of Mechanical Engineering, Tianjin University of Technology and Education, China

Abstract

To address the issues of discontinuous contact lines and sharp points on the tips of the gears in the cycloidal-involute rotor end profile of existing twin-screw vacuum pumps, a fully smooth rotor profile for twin-screw vacuum pumps is proposed. A concentric arc meshing model and a tip elliptical arc correction model are established, and the rotor profile equation is derived. Three-dimensional modeling is completed along with dynamic interference analysis. Furthermore, a comparative analysis of the rotor's geometric characteristics is conducted, focusing on aspects such as the leakage triangle and area utilization rate. The research results indicate that after the correction of the concentric arc meshing model, the area of the leakage triangle is reduced to 51.1% of that before correction, and the effective area utilization rate of the rotor end face is significantly improved.

Keywords

End Face Profile; Elliptical Arc; Concentric Circular Arc; Leakage Passage.

1. Introduction

If the 20th century was the era of oil vacuum pumps, then the 21st century is the century of dry vacuum pumps. With the growing industrial demand, China has continuously developed and produced various models of vacuum pumps[1-2]. Screw vacuum pumps have become the preferred vacuum equipment in industries such as microelectronics, semiconductor chips, and precision machining in Europe, America, and Japan, due to their compact structure, frictionless operation, wide pumping speed range, low noise, and oil-free operation[3-4]. With the progress of the times and the enhancement of environmental awareness, energy conservation and emission reduction have become global priorities. Achieving carbon peak and carbon neutrality goals, and promoting sustainable development, have become core issues in today's society. The development of oil-free vacuum pumps aligns with this mainstream trend of environmental protection and energy efficiency[5]. The screw rotor is a key component of screw vacuum pumps, directly affecting their performance and service life. The design of the rotor's cross-sectional profile is the focus of screw rotor research, as it directly impacts the pump's efficiency and manufacturing costs. As a result, screw pump manufacturers consider it a core secret[6-7]. Profile analysis plays a vital role in the design, performance optimization, fault diagnosis, and improvement of twin-screw vacuum pumps, as well as in research across various application fields. In-depth analysis of screw pump profiles can effectively enhance their performance and efficiency, meeting the diverse needs of different industries[8].

Zhang Shiwei and his team from Northeastern University[9-12] have made numerous achievements in the study of screw vacuum pump rotor end-face profile lines. They have analyzed some common issues of screw vacuum pumps and provided solutions. One of the solutions introduced is a twin-screw vacuum pump rotor profile line composed of cycloidal curves, root arcs, involute curves, and tooth top arcs. The design of this profile line, which is a combination of multiple curves, improves the pump's suction capacity and vacuum degree to some extent, while also reducing energy consumption and maintenance costs. However, this profile still faces issues such as discontinuous contact lines and difficulties in forming a stable meshing gap. Li Teng and his team from China University of Petroleum[13] designed a novel sine spiral-elliptical arc rotor and derived its profile equation. This design significantly enhances the performance of twin-screw vacuum pumps, but compared to traditional profiles, its structure is more complex, increasing the difficulty of rotor processing and making large-scale production challenging. Li Zhengqing and his team from Lanzhou Institute of Space Technology Physics[14] designed a smoothly connected cycloidal screw pump rotor profile line. This profile is a symmetric rotor profile with smooth transitions at the connections of each curve. This rotor can effectively reduce gas backflow during operation, but it does not show significant advantages in terms of volumetric efficiency.

The end profile of the rotor in a cycloidal-involute double screw pump typically consists of an outer cycloid, root circle, involute, and tip circle. This type of profile usually features three non-smooth sharp points. After the rotor is generated, sharp edges form, and the spatial contact line becomes discontinuous. Under the influence of pressure difference, gas leakage between adjacent working chambers occurs, creating a relatively large leakage path. During high-speed rotation of the rotor, friction and wear are likely to occur at the tooth tips, accompanied by noise, leading to damage to the rotor structure and causing the surface coating to peel off, thus affecting the overall performance of the twin-screw vacuum pump. Based on the cycloidal-involute profile, a fully smooth rotor end profile is proposed. A meshing model of concentric circular arcs with equal central angles and a tooth tip elliptical arc correction model are established to achieve a fully smooth transition of the profile, eliminating leakage paths and sharp points on the tooth tips. This results in reduced backflow and an improvement in the pump's vacuum performance.Design and Analysis of Fully Smooth Screw Rotor Profile Line.

2. Cycloidal-Involute Profile Line Analysis

Figure 1 shows a common cycloidal-involute profile, consisting of four segments of curves connected end to end. The involute, tooth top arc, long amplitude external cycloid, and root arc correspond to segments *AB, BC,CD*,and *DA* in the figure, respectively.

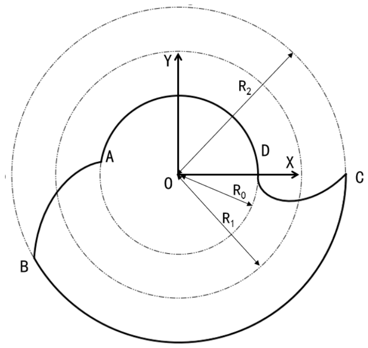

Figure 1. Cycloidal-Involute End-face Profile Line

As shown in Figure 1, let R_0 be the root circle radius, R_1 be the pitch circle radius, and R_2 be the top circle radius, with the following relationship:

$$R_1 = \frac{R_0 + R_2}{2} \tag{1}$$

As shown in Table 1, the meshing diagram and local profile diagram of the cycloidal-involute rotor, the existing cycloidal-involute linear connection at the root circle and involute transition forms a sharp point, creating a leakage channel. Additionally, after rotor generation, a sharp point forms at the connection between the outer cycloidal curve and the tooth tip circle. During high-speed rotor operation, this sharp point can lead to friction, causing damage to the rotor structure. Therefore, a chamfering treatment is required at this sharp point.

Table 1. The cycloidal-epicycloidal rotor meshing diagram and the local profile diagram

Existence of problems	Rotor Meshing Schematic	Local Profile Schematic
leakage passage	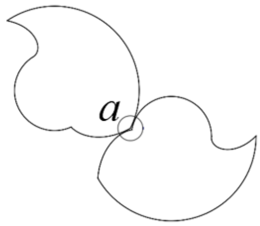	
sharp points	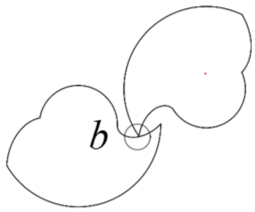	

2.1. Analysis of the Endface Profile of the Fully Smooth Roto

Based on the cycloidal-involute rotor end-face profile, a novel fully smooth twin-screw rotor end-face profile is proposed, as shown in Figure 2(a). The rotor end-face profile consists of a sequence of transition arcs *AB*, involute *BC*, transition arcs *CD*, tooth tip arcs *DE*, tooth tip elliptical arcs *EF*, external cycloid *FG*, root arcs *GA*, and a seven-segment curve. The main feature of the new rotor end profile is: two segments of concentric circular arcs with equal central angles, one segment of elliptical arc, and a smooth transition tangent to the outer cycloid, achieving a fully smooth transition of the profile. This design eliminates leakage paths and sharp points on the tooth tip contours, thereby improving the operating speed and ultimate vacuum of the vacuum pump.

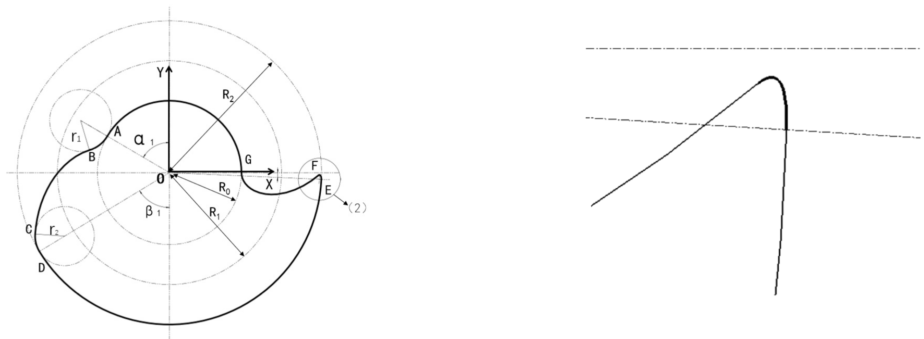

(a) The end-face profile of the fully smooth rotor **(b)** Elliptical arc.

Figure 2. Profile diagram of the fully smooth rotor end-face contour and Elliptical arc.

2.1.1. Tooth Tip Elliptical Arc Correction Model

The elliptical arc tooth tip modification profile is shown in Figure 3. The semi-minor axis of the ellipse is denoted as *b*, and the semi-major axis as *a*. The semi-minor axis is aligned with the radius direction of the tooth top circle R_2 meaning the center of the ellipse is located at a distance of R_2-b from the center of the tooth top circle. Points *E* and *F* are tangent to the tooth top circle and the external cycloid of the major profile, respectively. The coordinates of point *F* are (x_1,y_1). The specific parametric equations are as follows:

$$x_{EF} = (R_2 - b) + b\cos t$$
$$y_{EF} = a\sin t \tag{2}$$

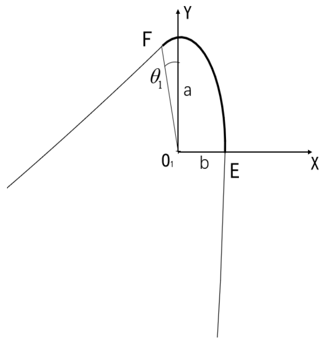

Figure 3. Tooth tip elliptical arc modification

In which, the t range of values for t is $\left[0, \frac{\pi}{2} + \theta_1\right]$, $\theta_1 = \frac{\pi}{2} + \arctan\frac{x_1}{y_1}$.

2.1.2. Nolute and its Conjugate Curve

The analysis of the involute of the screw rotor BC is shown in Figure 4. The involute BC rolls on the base circle with radius R_i and center O_1 in the $X_1O_1Y_1$ plane, and its parametric equation is as follows:

$$x_{BC} = R_i\cos(\lambda - \lambda_0) + R_i\lambda\sin(\lambda - \lambda_0)$$
$$y_{BC} = R_i\sin(\lambda - \lambda_0) - R_i\lambda\cos(\lambda - \lambda_0) \tag{3}$$

The radius of the base circle of the involute is R_i=R_0, where λ_0 is the initial turning angle of the involute, λ_1 is the initial value of the involute's unwrapped angle, and λ_2 is the maximum value of the involute's unwrapped angle.

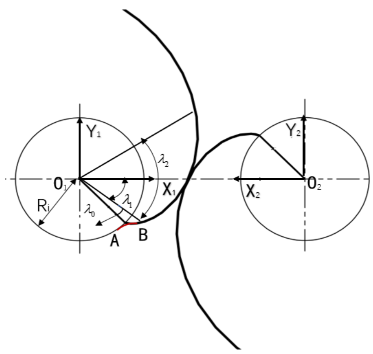

Figure 4. Involute curve and its conjugate profile

Since the pitch circle radii of the two screw rotors are identical, the transmission ratio of the two screw rotors is 1:1. Additionally, the base circle radii of the male and female rotors are also the same. Therefore, the involute in $X_1O_1Y_1$ and the involute in $X_2O_2Y_2$have identical shapes. Their conjugate curves transform into involutes in $X_2O_2Y_2$, and the parametric equations of the involute in $X_2O_2Y_2$ are exactly the same as those of the involute in $X_1O_1Y_1$.

2.1.3. Long-profile Epitrochoid and its Conjugate Curve

The analysis of the long-length outer cycloid GF of the screw rotor is shown in Figure 5. The long-length outer cycloid is generated when a moving circle rolls externally along a fixed circle (base circle) in pure rolling without slipping. The trajectory is traced by a point rigidly connected to the center of the moving circle, located outside the moving circle. Its parametric equation is as follows:

$$x_{GF} = 2(r_i + l)\cos\varphi - R_2\cos 2\varphi$$
$$y_{GF} = 2(r_i + l)\sin\varphi - R_2\sin 2\varphi \tag{4}$$

r_i is the radius of the rolling circle, l is the distance from the moving point to the circumference of the rolling circle, R_2 is the radius of the tip circle, and the value range of φ is $0 \le \varphi \le \frac{\pi}{2} - \varphi_1$.

The end face profiles of the two rotors are identical in shape and size, and the rotor transmission ratio is 1:1. Their conjugate profiles are transformed into long arc cycloids in the $X_2O_2Y_2$ coordinate system, with the parametric equation being the same as that of the long arc cycloid in the $X_1O_1Y_1$ coordinate system.

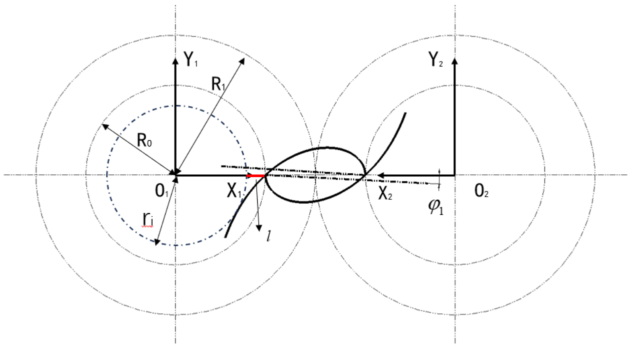

Figure 5. shows the epicycloid and its conjugate curve

2.1.4. Analysis of the Root Circle, Crest Circle, and Transition Arc Profile

As shown in Figure 2(a), the curve *GA* is a tooth tip circular arc with radius R_0, centered at *O*. Its profile parametric equation is given by:

$$x_{GA} = R_0\cos\alpha$$
$$y_{GA} = R_0\sin\alpha \tag{5}$$

The curve *DE* is a root circle arc with a radius of R_2, centered at *O*. Its profile parametric equation is as follows:

$$x_{DE} = R_2\cos\beta$$
$$y_{DE} = R_2\sin\beta \tag{6}$$

The transition circular arc *AB* is a segment of a circle with radius r_1. Its parametric equation is as follows:

$$x_{AB} = (R_0 + r_1)\sin\alpha_1 + r_1\cos\xi$$
$$y_{AB} = (R_0 + r_1)\cos\alpha_1 + r_1\sin\xi \tag{7}$$

The transition circular arc *CD* is a segment of a circle with a radius r_2. Its curve's parametric equation is as follows:

ISSN: 2688-8645

$$x_{CD} = (R_2 - r_1)\sin\beta_1 + r_1 \sin\xi$$
$$y_{CD} = (R_2 - r_1)\cos\beta_1 + r_1 \cos\xi \quad (8)$$

As shown in Figure 6, the two transition circular arcs have equal central angles, denoted as ξ. A stable meshing gap can be formed between the arcs *AB* and *CD.* The meshing gap between the two circular arcs is the difference in their radii, denoted as $\Delta = r_1 - r_2$.

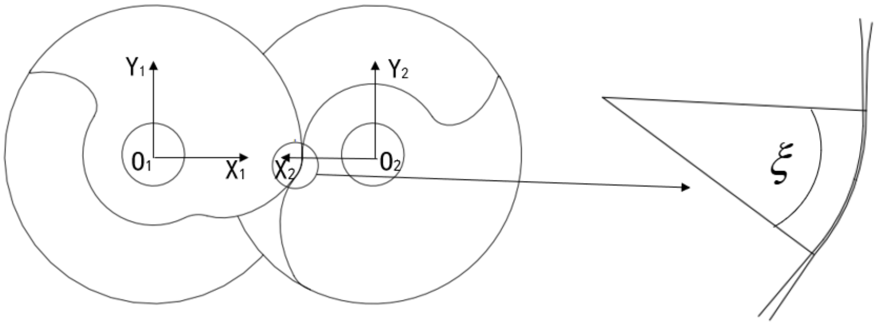

Figure 6. Concentric circular arc meshing model

3. Modeling and Geometric Characterization of the Fully Smooth Screw Rotor

This section will focus on the modeling of the new type of fully smooth screw rotor end face profile and dynamic interference analysis. Additionally, a comparative geometric analysis will be conducted in terms of rotor end face meshing lines, leakage triangles, and rotor end face area utilization.

3.1. Modeling of a Novel Fully-smooth Twin-screw Rotor

As shown in Figure 7(a), the equidistant screw rotor is generated by a new type of profile curve that spirals along the axial direction. During the generation process, when the rotational speed of the screw and the rate of spiral ascent maintain a constant ratio, the parameters of the constituent curves of the profile remain constant, with each curve having a fixed set of values. The profile design of these curves is an equidistant section profile, and there is no variation in parameters throughout the entire process. A pair of screw rotors generated using the new smooth rotor section profile is shown in Figure 7(b). Through the rotor shaft, synchronization of the male and female rotors can be achieved using the meshing-gear command.

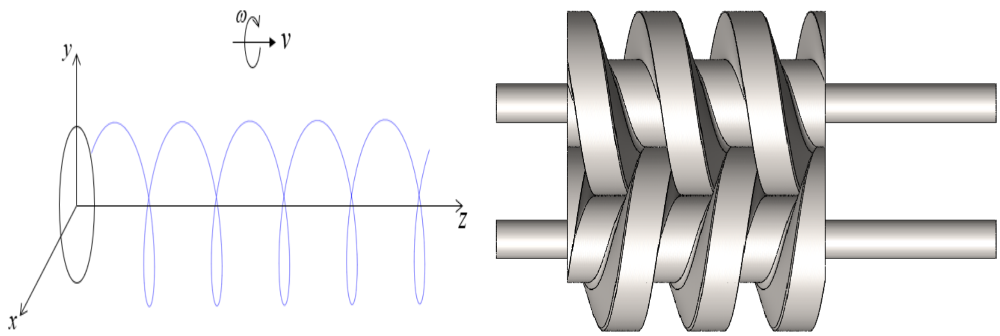

(a) Scanning path **(b)** Modeling of the equidistant screw rotor

Figure 7. Cross-sectional profile scanning path and equidistant screw rotor modeling

Dynamic interference analysis was conducted using the 3D modeling software SOLIDWORKS to observe the meshing conditions. Based on the observations, it was found that no interference occurs during the rotation of the rotor, and the two rotors achieve complete and correct meshing, maintaining a stable meshing clearance. The envelope trajectory of the rotor cross-sectional profile is shown in Figure 8.

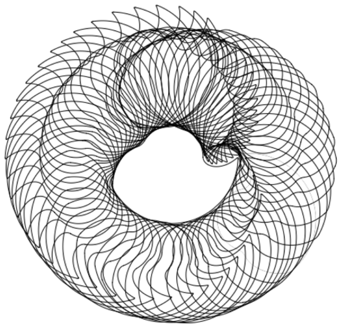

Figure 8. Enveloping trajectory of the sectional profile

The specific parameters of the new fully smooth twin-screw rotor are shown in Table 2.

Table 2. Parameters of the novel fully smooth twin-screw rotors.

Root circle radius	Radius of the tooth top circle	Length of the spatial contact lin	Effective utilization of area
9mm	19mm	110.78mm	0.586mm^2

3.2. Comparison of Leakage Triangular Model

Gas leaks through the leakage triangle from the high-pressure working chamber to the adjacent low-pressure working chamber. The area of the leakage triangle affects the operating efficiency and leakage rate of the twin-screw vacuum pump. The effective area of the gas flow perpendicular to the leakage triangle is a key factor influencing the leakage rate. As shown in Figure 9 (a) and (b), the leakage triangle area of the new fully smooth rotor is significantly smaller compared to the existing rotors, playing a crucial role in improving the vacuum pump's operating efficiency and reducing the leakage rate.

(a) Existing rotor leakage triangle **(b)** Fully smooth rotor leakage triangle

Figure 9. Comparison of leakage triangles

The area of the leakage triangle is presented in Table 3. After the arc modification, the leakage triangle area is reduced to 51.1% of the unmodified value, effectively decreasing the leakage.

Table 3. Comparison of leakage triangular area

	The existing rotor	Fully smooth rotor
Leakage triangle area S/mm^2	1.6857	0.8615

3.3. Area Utilization Efficiency

As shown in Figure 10, the difference between the area of the "∞"shaped pump chamber cross-section and the area enclosed by the screw rotor end face profile, along with the total pump chamber cross-sectional area, is illustrated. The shaded area represents the rotor cross-sectional area, while the unshaded area corresponds to the gas flow through the pump chamber cross-sectional area. The rotor area utilization coefficient of the twin-screw vacuum pump is denoted by *C*, and the formula can be defined as:

$$C = \frac{S_C}{S_A} \times 100\% = \frac{S_A - 2S_{B_1}}{S_A} \times 100\% \tag{9}$$

The formula for the total cross-sectional area of the pump chamber is as follows:

$$S_A = 2\pi R_2{}^2 - 2R_2(R_2 \arccos\frac{R_1}{R_2} - R_1 \sin(\arccos\frac{R_1}{R_2})) \tag{10}$$

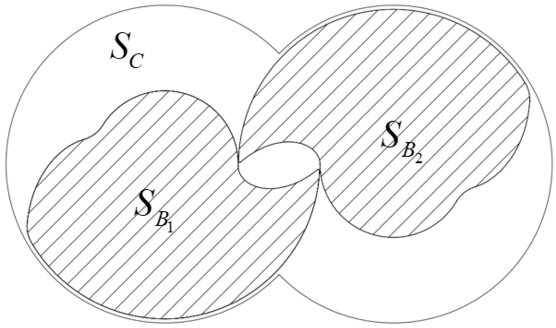

Figure 10. Pump chamber cross-sectional area

S_{B_1} and S_{B_2} represent the cross-sectional areas of the male and female rotors, respectively. Since the end profile of the rotor is composed of multiple segments of smooth arcs that are connected end-to-end, and given the known geometric parameters of the rotor and the equation of the profile for each segment, the area enclosed by each segment of the arc in the Cartesian coordinate system can be determined through analytical methods to simplify the calculation.

$$S_i = \int x_i y_i{}^2 - x_i{}^2 y_i d\partial \tag{11}$$

In this context, S_i represents the area enclosed by each segment of the arc in the Cartesian coordinate system.

4. Conclusion

1.A new fully smooth rotor profile for a twin-screw vacuum pump is proposed, incorporating a tooth tip elliptical arc correction model. A meshing model of concentric circular arcs is established, and an elliptical arc is applied to the tooth tips of the screw rotor, achieving a fully smooth transition of the rotor end profile.

2.The rotor was modeled and a dynamic interference check was performed. The results indicate that the fully smooth rotor profile achieves correct meshing and provides a stable meshing gap. Additionally, a comparative analysis based on the geometric characteristics of the leakage triangle and area utilization rate demonstrated that the new tooth tip elliptical arc correction model for the twin-screw vacuum pump's fully smooth rotor profile has significant advantages in terms of obtaining a stable meshing gap and reducing leakage area.

ISSN: 2688-8645

References

[1] Shengping Gao, Jianping Cao, Qingkun Meng, et al. The Current Status of Screw Pump Standardization in China and Discussion on International Standardization. Petroleum Industry Technical Supervision, 2012, 28(07): 15-19.

[2] Dong Yong. Dry Pumps: A New Star Shining on the Vacuum Industry in the 21st Century [J]. Vacuum, 1997 (04): 52-55.

[3] Jinliang Tuo;Bei Guo;Rui Wu;Yu Zhang;Xiaole Chen. Study on the performance prediction of dry twin screw vacuum pump[J]. IOP Conference Series: Materials Science and Engineering.Volume 425 , Issue 1.2018.

[4] Hailei Wang, Zhao Ye. Characteristics and Applications of Screw Vacuum Pumps [J]. Scientist, 2017, 5 (11): 102-103.

[5] Sun Kun, Li Kun, Senhui Wang, et al. Design and Strategies of Screw Vacuum Pumps under the 'Dual Carbon' Vision [J]. Vacuum, 2023, 60(01): 57-61.

[6] Shihwei Zhang, Zhao Fan, Zhang Jie, et al. Review and Outlook on the Design Concept of Screw Rotors for Oil-Free Screw Vacuum Pumps [J]. Vacuum, 2015, 52(05): 1-12.

[7] Zheng-Xiang Zhang;Zhang-Hua Fong. A novel tilt form grinding method for the rotor of dry vacuum pump[J]. Mechanism and Machine Theory. Volume 90, Issue . 2015 . PP 47-58.

[8] Gao L, Zhao Y, Chen Y, et al. Development of Roots-Screw Integrated Oil-Free Vacuum Pump [C]// Chinese Vacuum Society. Proceedings of the 10th Asian and Australian Vacuum and Surface Science Conference, Chinese Vacuum Society 2021 Annual Academic Conference, and the 15th International Conference on Vacuum Science and Engineering Applications. [Publisher Unspecified], 2021: 2.

[9] Shiwei Zhang, Chenghai Xu, Kuizhi Guan. Study on the Rotor Profile of Single-Head Variable Pitch Screw in Screw Vacuum Pumps [J]. Vacuum, 2002, (02): 9-11.

[10] Shiwei Zhang, Liang Wensheng, Zhao Yu, et al. A Practical Oil-Free Screw Vacuum Pump with Single-Head Equal Pitch Rotor Profile [C]//Chinese Vacuum Society. Proceedings of the 2008 Annual Conference of the Chinese Vacuum Society. 2008: 1.

[11] Shiwei Zhang,Zhijun Zhang,and Chenghai Xu.Virtual Design and Structural Optimization of Dry Twin Screw Vacuum Pump with a New Rotor Profile[J]. Applied Mechanics and Materials Vols. 16-19 (2009) pp 1392-1396.

[12] Shiwei Zhang, Sun Kun, Han Feng. Analysis of Common Problems in the Design of Screw Vacuum Pumps [J]. Vacuum, 2021, 58(01): 23-28.

[13] Li Teng, Xiehao Zhao, Wang Jun, et al. Design and Simulation of a New Elliptic Arc Corrected Sine Spiral Rotor for the Twin-Screw Vacuum Pump [J]. Journal of Vacuum Science and Technology, 2023, 43 (10): 841-847.

[14] Zhengqing Li, Xianhu Han, Yuhong Cai, et al. Design and Analysis of the Cycloidal Rotor Profile for Smoothly Connected Screw Vacuum Pump [J]. Vacuum and Cryogenics, 2023, 29(02): 117-120.